COMPDYN 2015
5th ECCOMAS Thematic Conference on
Computational Methods in Structural Dynamics and Earthquake Engineering
M. Papadrakakis, V. Papadopoulos, V. Plevris (eds.)
Crete Island, Greece, 25–27 May 2015

PRELIMINARY INVESTIGATIONS OF THE LOW-VELOCITY IMPACT RESPONSE OF A SMART TRIMORPH PLATE FOR ACTIVE DAMAGE MITIGATION

Akuro Big-Alabo[1], Philip Harrison[2], and Matthew P. Cartmell[3]

[1] University of Glasgow
Systems, Power and Energy Research Division, School of Engineering, G12 8QQ, Scotland, UK
e-mail: a.big-alabo.1@research.gla.ac.uk

[2] University of Glasgow
Systems, Power and Energy Research Division, School of Engineering, G12 8QQ, Scotland, UK
e-mail: Philip.Harrison@glasgow.ac.uk

[3] University of Sheffield
Department of Mechanical Engineering, Mappin Street, Sheffield, S1 3JD, England, UK
e-mail: m.cartmell@sheffield.ac.uk

Keywords: Trimorph plate, Low-velocity impact, Elastoplastic contact model, Impact damage, Active damage mitigation.

Abstract. *The elastoplastic impact response of a trimorph plate subjected to low-velocity large mass impact has been investigated using analytical models. In formulating the impact model, the displacement of the impactor, vibration of the plate and local contact mechanics were accounted for. The vibration of the trimorph plate was modelled using the classical laminate plate theory, while the local contact mechanics was modelled using a Meyer-type compliance model that accounts for post-yield effects in the loading and unloading stages of the impact. The impact model is a set of coupled nonlinear differential equations and was solved using the NDSolve function in Mathematica™. Both the modelling and solution approach were validated using a benchmark case study. Investigations were carried out for an Al/PVDF/PZT trimorph plate configuration. Contrary to the general position in the literature that the response of a large mass impact is insensitive to the compliance model used to estimate the impact force [1], the simulations of the present impact model show that the indentation history was sensitive to the compliance model used. Also, the elastoplastic compliance model predicted a permanent indentation which the elastic compliance model cannot estimate. Therefore, the use of elastoplastic compliance models in large mass impact analysis is imperative. Finally, the application of a smart trimorph plate with piezoelectric actuator layer for active mitigation of impact damage was discussed.*

1 INTRODUCTION

Transversely flexible plates (i.e. plates that could bend in the direction perpendicular to their plane) are used in many structural applications (e.g. building panels, car and airplane bodies, ceilings and floorings) in environments where they can be exposed to damage due to impact by blunt projectiles. Therefore, a good understanding of the response of transversely flexible plates to blunt object impact is necessary for design decision-making, damage diagnosis, and active control of impact response. The response of a transversely flexible plate to a blunt object impact is governed by the interaction between flexural oscillations and local indentation of the plate [2]. The simplest analytical cases of transversely flexible plate impacts are the asymptotic cases of the infinite plate response and the quasi-static bending response. Each of these asymptotic cases is modelled by a single differential equation [3]. In general, the model for the impact response of a transversely flexible plate is a set of coupled differential equations that accounts for the flexural oscillations of the plate, the displacement of the impactor and the local indentation. This model has been referred to as the complete model [3] and is applied in the present study to investigate the impact response of a transversely flexible laminated plate structure.

Analytical studies of the normal impact of rigid spheres on transversely flexible monolithic and laminated rectangular plates abound in the literature. Most of these studies deal with elastic impact [1, 2, 4, 5] and those that deal with elastoplastic impact use simplified models for the elastoplastic indentation [6 – 9] that may introduce significant errors in the prediction of the impact response of the plate [6]. The use of well validated elastoplastic contact models in the complete modelling approach is quite challenging computationally, but has the advantage of producing more reliable results and providing details of the impact response that would not have been obtained otherwise. Hence, analytical models that are capable of predicting the elastoplastic response of a transversely flexible plate exposed to impact of a blunt projectile are desirable.

In this paper, analytical models have been derived to investigate the elastoplastic response a transversely flexible trimorph plate subjected to low-velocity, large mass impact. A trimorph plate is defined as a general three-layer laminated plate in which each layer is made of a different material [10]. An example of the application of the trimorph plate configuration is the integration of sensor and actuator layers to a host layer for the purpose of active sensing and control of the plate response. The analytical models for the impact response of the trimorph plate are formulated using the classical laminate plate theory (CLPT) and an elastoplastic contact model that accounts for post-yield effects in the loading and unloading stages. The impact models are used to study the impact response of an Al/PVDF/PZT trimorph plate configuration. The rest of the paper is structured as follows: first, the analytical models for analysis of the impact response of the trimorph plate are formulated; secondly, the expressions for determination of the material properties of the trimorph plate are presented and discussed; thirdly, results from simulations of the analytical models are discussed; fourthly, the feasibility of active damage mitigation using a smart trimorph plate is discussed; and finally, the conclusions of the present study are discussed.

2 IMPACT MODEL OF TRIMORPH PLATE

The impact system studied is a rectangular trimorph plate that is simply supported on all sides and subjected to the transverse elastoplastic impact of a rigid mass with spherical contact surface. The point of impact is at the centre of the plate. It is assumed that the layers of the trimorph plate are perfectly bonded and each layer is made up of an isotropic material. Figure 1 shows a sketch of the impact system with the layers of the trimorph plate having

different shading patterns to indicate different material make-up. This section presents the formulation of the analytical models used for investigation of the trimorph plate. First, the model for transverse vibration of the trimorph plate is derived based on the CLPT. Next, the elastoplastic contact model used to estimate the impact force and account for the local deformation is presented. The section concludes with a combination of the vibration and contact models to formulate an elastoplastic impact model for the trimorph plate.

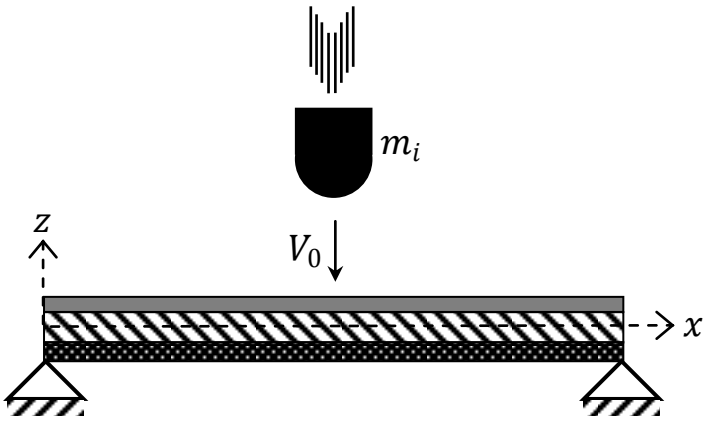

Figure 1: Impact of a trimorph plate by a spherical projectile.

2.1 Vibration model for thin rectangular trimorph plate

The transverse oscillations or vibrations of a thin rectangular plate can be accurately modelled using the classical plate theory (CPT). A thin plate is one in which the thickness to length ratio is less than or equal to 0.1 [11]. When the amplitude of the transverse vibration of the plate is small in comparison to the thickness of the plate, the effect of in-plane forces arising from membrane stretching can be neglected, and the equation for transverse vibration of the plate according to the CPT is given as [1]:

$$\frac{\partial^2 M_x}{\partial x^2} + 2\frac{\partial^2 M_{xy}}{\partial x \partial y} + \frac{\partial^2 M_y}{\partial y^2} = \rho h \frac{\partial^2 w}{\partial t^2} - q(x, y, t) \tag{1}$$

where M_x, M_{xy}, and M_y are moment resultants, $w = w(x, y, t)$ is the transverse displacement, and $q(x, y, t)$ is the transverse excitation. The moment resultants can be determined from the constitutive equations derived using the classical laminated theory (CLT). The constitutive equations for a thin trimorph plate with isotropic layers have been derived based on the CLT in reference [10], and from these equations the moment resultants are given as:

$$\begin{matrix} M_x \\ M_y \\ M_{xy} \end{matrix} = \begin{bmatrix} B_{11} & B_{12} & 0 & \varepsilon_x^0 \\ B_{12} & B_{11} & 0 & \varepsilon_y^0 \\ 0 & 0 & B_{66} & \varepsilon_{xy}^0 \end{bmatrix} + \begin{bmatrix} D_{11} & D_{12} & 0 & k_x^0 \\ D_{12} & D_{11} & 0 & k_y^0 \\ 0 & 0 & D_{66} & k_{xy}^0 \end{bmatrix} \tag{2}$$

where $[B_{ij}]$ and $[D_{ij}]$ are the extension-bending and pure bending stiffness matrices respectively, $\{\varepsilon_x^0 \;\; \varepsilon_y^0 \;\; \varepsilon_{xy}^0\}^T$ is the strain vector, and $\{k_x^0 \;\; k_y^0 \;\; k_{xy}^0\}^T$ is the curvature vector. The subscript '0' indicates mid-plane strains and curvatures. The expressions for determination of the elements of the stiffness matrices are discussed in Section 3. The elements of both the strain and curvature vectors can be expressed in terms of the displacements of the mid-plane as shown.

$$\varepsilon_x^0 = \frac{\partial u^0}{\partial x}; \quad \varepsilon_y^0 = \frac{\partial v^0}{\partial y}; \quad \varepsilon_{xy}^0 = \frac{\partial u^0}{\partial y} + \frac{\partial v^0}{\partial x}$$
$$k_x^0 = -\frac{\partial^2 w}{\partial x^2}; \quad k_y^0 = -\frac{\partial^2 w}{\partial y^2}; \quad k_{xy}^0 = -2\frac{\partial^2 w}{\partial x \partial y} \tag{3}$$

The combination of the constitutive equations derived using the CLT and the equations of motion derived using the CPT is called the classical laminate plate theory. Substituting equations (2) and (3) in equation (1) and neglecting in-plane displacements, the governing equation for the transverse vibration of the trimorph plate is derived thus:

$$\rho h \frac{\partial^2 w}{\partial t^2} + D_{11} \left(\frac{\partial^4 w}{\partial x^4} + \frac{\partial^4 w}{\partial y^4} \right) + 2(D_{12} + 2D_{66}) \frac{\partial^4 w}{\partial x^2 \partial y^2} = q(x, y, t) \tag{4}$$

The transverse displacement and excitation can be expressed in series form as:

$$w(x, y, t) = \sum_{m=1}^{\infty} \sum_{n=1}^{\infty} W_{mn}(t) X_m Y_n \tag{5a}$$

$$q(x, y, t) = \sum_{m=1}^{\infty} \sum_{n=1}^{\infty} Q_{mn}(t) \sin\left(\frac{m\pi x}{a}\right) \sin\left(\frac{n\pi y}{b}\right) \tag{5b}$$

In equation (5b), $Q_{mn}(t)$ is the load coefficient determined as:

$$Q_{mn}(t) = \frac{4}{ab} \int_0^a \int_0^b q(x, y, t) \sin\left(\frac{m\pi x}{a}\right) \sin\left(\frac{n\pi y}{b}\right) dx dy \tag{6}$$

X_m and Y_n are admissible shape functions that satisfy the boundary conditions but not necessarily the PDE. Equation (4) can be reduced to an ODE using the Galerkin variation approach [11]. The vibration model (equation (4)) has been presented in such a way that the LHS of the equation is a partial differential expression (*PDEx*) in terms of the transverse displacement and the RHS is the external excitation. Thus the Galerkin variation formula for derivation of the reduced model can be expressed as:

$$\int_0^b \int_0^a \left(PDEx - q(x, y, t) \right) X_m Y_n dx dy = 0 \tag{7}$$

Equation (7) can be evaluated for any boundary condition but the present analysis has been limited to simply-supported boundary conditions on all edges of the rectangular plate (SSSS) for mathematical convenience, and without loss of generality. For SSSS, the shape functions can be expressed as $X_m = \sin(m\pi x/a)$ and $Y_n = \sin(n\pi y/b)$. Substituting equations (4), (5a) and (5b) in equation (7) and evaluating the resulting double integral for SSSS, the reduced model for small transverse oscillations of the trimorph plate is:

$$\ddot{W}_{mn} \} + K\{W_{mn}\} = F(t)\{\gamma_{mn} \tag{8}$$

where $W_{mn}(t)$ is the time-domain transverse displacement of the (m, n) vibration mode;

$K = \frac{\pi^4}{\rho h}\left[D_{11} \left(\frac{m^4}{a^4} + \frac{n^4}{b^4} \right) + \frac{2m^2 n^2 (D_{12} + 2D_{66})}{a^2 b^2} \right]$ is the mechanical bending stiffness per unit mass;

$F(t)$ is the transverse excitation; and γ_{mn} is a constant derived from the evaluation of equation (6). Considering an excitation that is applied at a point (x_0, y_0) then,

$$\gamma_{mn} = \frac{4}{\rho hab} \text{Sin}\left(\frac{m\pi x_0}{a}\right) \text{Sin}\left(\frac{n\pi y_0}{b}\right. \tag{9}$$

where ρ is the density of the plate; h is the total thickness of the plate; a and b are the planar dimensions of the plate.

2.2 Elastoplastic contact model

Static contact models can be used to estimate the impact force during low-velocity impact of a transversely flexible plate [1, 2]. The low-velocity impact of a transversely flexible plate often results in elastoplastic indentation at the point of impact. In such cases, the use of Hertz contact model or linearised elastoplastic contact models to estimate the impact force introduces significant errors in the predicted impact response [6, 9]. Recently, Big-Alabo et al [12, 13] developed an elastoplastic contact model in which all of the loading and unloading stages are modelled using Meyer-type compliance models. The main advantages of the elastoplastic model are its simplicity and computational tractability when used for impact analysis [12]. Details of the formulation of the elastoplastic model can be found in [12, 13]. This elastoplastic contact model has been used in the present impact analysis with a slight modification in the expression for the unloading stage as explained below. The contact model has four loading stages consisting of one elastic loading stage, two elastoplastic loading stages and one fully plastic loading stage. Also, there is a single unloading (restitution) stage. The elastoplastic contact model is given as follows.

Elastic loading stage

$$F_e = K_h \delta^{3/2} \qquad 0 \le \delta \le \delta_y \tag{10}$$

where F_e is the elastic loading force, and K_h is the Hertzian contact stiffness calculated as $K_h = (4/3)ER^{1/2}$. The constants E and R are the effective modulus and radius respectively, and are calculated as: $E = [(1-\upsilon_i^2)/E_i + (1-\upsilon_t^2)/E_t]^{-1}$ and $R = [1/R_i + 1/R_t]^{-1}$. The subscripts i and t stand for indenter and target respectively, and υ is the Poisson's ratio.

Elastoplastic loading stages

- Region I: Nonlinear elastoplastic loading

$$F_{ep}^{I} = K_h\left(\delta - \delta_y\right)^{3/2} + K_h\delta_y^{3/2} \qquad \delta_y \le \delta \le \delta_{tep} \tag{11}$$

where F_{ep}^{I} is the nonlinear elastoplastic loading force, and δ_y is the indentation at yield. The expression for calculating δ_y is given as: $\delta_y = \left(1.1\pi RS_y/K_h\right)^2$ where S_y is the yield stress of the target.

- Region II: Linear elastoplastic loading

$$F_{ep}^{II} = K_l\left(\delta - \delta_{tep}\right) + K_h\left[\left(\delta_{tep} - \delta_y\right)^{3/2} + \delta_y^{3/2} \qquad \delta_{tep} \le \delta \le \delta_p \right. \tag{12}$$

where F_{ep}^{II} is the linear elastoplastic loading force, K_l is the linear contact stiffness in Region II, δ_{tep} is the indentation at the transition between Regions I and II. The constants in equation (12) are determined as: $K_l = 5.40K_h\delta_y^{1/2}$ and $\delta_{tep} = 13.93\delta_y$.

Fully plastic loading stage

$$F_{fp} = K_p\left(\delta - \delta_p\right) + F_{\delta=\delta_p} \qquad \delta_p \le \delta \le \delta_m \tag{13}$$

where F_{fp} is the fully plastic loading force, K_p is the linear contact stiffness during the fully plastic loading stage, δ_p is the indentation at the onset of fully plastic loading and $F_{\delta=\delta_p}$ is the

value of the contact force at δ_p. The constants in equation (13) are determined as: $K_p = 4.6\pi RS_y$; $\delta_p = 82.5\delta_y$; and $F_{\delta=\delta_p} = 70.0K_l\delta_y + 47.6K_h\delta_y^{3/2}$.

Unloading (restitution) stage

$$F_u = K_u\left(\delta - \delta_f\right)^{3/2} \qquad \delta_f \le \delta \le \delta_m \tag{14}$$

where F_u is the elastic unloading force, K_u is the nonlinear contact stiffness during unloading, and δ_f is the fixed or permanent indentation at the end of the unloading. The constants in equation (14) are determined as: $K_u = (4/3)ER_d^{1/2}$ and $\delta_f = \delta_m - \left(3F_m/4ER_d^{1/2}\right)^{2/3}$ where R_d is the deformed effective radius, and $R_d \ge R$; δ_m and F_m are the indentation and force at the end of the loading. For a half-space impact the end of the loading response coincides with the point when the maximum indentation occurs, but this is not necessarily so for transversely flexible plate impact [1]. Nevertheless, the impact loading ends when the velocity of the impactor is zero for both half-space impact and transversely flexible plate impact.

Whereas the Hertz stiffness is related to the effective radius, the unloading stiffness is related to a deformed effective radius due to plastic deformation effects [13]. In references [12, 13] R_d was determined as: $R_d \cong R$ when the maximum penetration is in the elastoplastic loading regime or the initial phase of the fully plastic loading regime; and $R_d \cong R + \delta_m/2$ when the maximum penetration is well into the fully plastic loading regime e.g. $\delta_m/\delta_p \ge 2$. The approximations used in [12] could lead to an underestimation of the permanent indentation at the end of the unloading. Based on published observations of the unloading response during elastoplastic indentation [14 – 16], the expressions in equation (15) are proposed here to calculate R_d. A comparison of the unloading response predicted using equation (15) and the expressions in [12] against published experimental data [17] is shown in Figure 2, and equation (15) is seen to give a better prediction of the experimental data.

$$\begin{aligned}
R_d &= R && 0 \le \delta_m \le \delta_y \\
R_d &= \left[\left(\frac{\delta_m - \delta_y}{\delta_{tep} - \delta_y}\right)^{3/2} + 1\right]R && \delta_y \le \delta_m \le \delta_{tep} \\
R_d &= \left[0.8\left(\frac{\delta_m - \delta_{tep}}{\delta_p - \delta_{tep}}\right) + 2\right]R && \delta_{tep} \le \delta_m \le \delta_p \\
R_d &= 2.8R && \delta_m > \delta_p
\end{aligned} \tag{15}$$

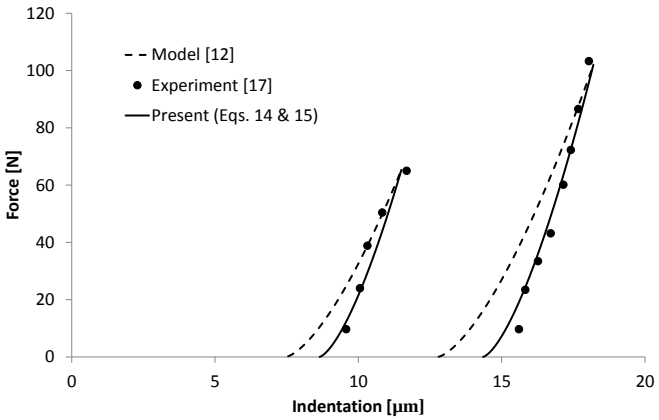

Figure 2: Unloading response during static indentation of AISI steel by a spherical tungsten carbide indenter.

2.3 Impact model for thin rectangular trimorph plate

During transversely flexible plate impact the local indentation of the plate is defined as the difference between the displacements of the impactor and plate [1], with the former being larger. When the displacement of the plate is equal to or higher than that of the impactor, contact between the plate and the impactor ceases. Assuming the displacement of the impactor is designated as $w_i(t)$ then, the local indentation can be expressed as:

$$\delta(t) = w_i(t) - w(t) \tag{16}$$

The equation of motion for the impactor can be expressed as:

$$\ddot{w}_i = -F(t)/m_i \tag{17}$$

where m_i is the mass of the impactor and $F(t)$ is the impact force, which is estimated using the elastoplastic contact model presented in sub-section 2.2. Equations (8), (10) – (14), and (17) form the complete impact model for analysis of the trimorph plate. These equations produce a set of P + 1 coupled ODEs in each impact stage that must be solved simultaneously; P represents the number of vibration modes used in the solution. For impact at the centre of the plate (i.e. $x_0 = a/2$ and $y_0 = b/2$), $P = (m+1)(n+1)/4$ where $m, n = 1, 3, 5, \ldots$ are odd integers.

3 DETERMINATION OF MATERIAL PROPERTIES OF TRIMORPH PLATE

The trimorph plate is a composite laminate in which each layer has different material properties. To solve the impact model formulated in Section 2 the material properties of the trimorph plate must be determined. In this section, the material properties of the trimorph plate are obtained using analytical techniques.

3.1 Stiffness of the trimorph plate

The bending-extension and bending stiffness elements are determined from the CLT as:

$$B_{ij} = \frac{1}{2}\sum_{k=1}^{L} \bar{Q}_{ijk}\,(z_k^2 - z_{k-1}^2 \quad ; \; D_{ij} = \frac{1}{3}\sum_{k=1}^{L} \bar{Q}_{ijk}\,(z_k^3 - z_{k-1}^3 \tag{18}$$

where L is the total number of layers; $\bar{Q}_{ijk}$ is the transformed reduced stiffness of the kth layer of the laminate, and is obtained from the material properties of the kth layer as shown in [10]. Staab [18] presented alternative expressions to equations (18), and the stiffness coefficients were expressed in terms of lamina thickness and the distance of the lamina centroid measured from the mid-plane. Here, simpler expressions are derived to express the stiffness coefficients in terms of lamina thickness and the total thickness of the laminate.

From Figure 3, the following can be deduced geometrically: $z_k - z_{k-1} = h_k$; $z_k = \sum_{i=1}^{k} h_i - h/2$ for $k > 0$ or $z_{k-1} = \sum_{i=1}^{k-1} h_i - h/2$ for $k > 1$; where h_k is the thickness of the kth layer. If the conditions stated are not satisfied then, $z_k = 0$ or $z_{k-1} = 0$ respectively. The quadratic expression of the B_{ij} elements can be expanded as:

$z_k^2 - z_{k-1}^2 = (z_k + z_{k-1})(z_k - z_{k-1}) = (z_k - z_{k-1} + 2z_{k-1})(z_k - z_{k-1}$

Therefore, $z_k^2 - z_{k-1}^2 = (h_k + 2z_{k-1})h_k = h_k\big(h_k + 2\sum_{i=1}^{k-1} h_i - h\big)$.

Also, $z_k^3 - z_{k-1}^3 = (z_k - z_{k-1})^3 + 3(z_k - z_{k-1})z_k z_{k-1}$.

Therefore, $z_k^3 - z_{k-1}^3 = h_k^3 + 3h_k \quad \sum_{i=1}^{k} h_i - h/2\big) \quad \sum_{i=1}^{k-1} h_i - h/2\big)$.

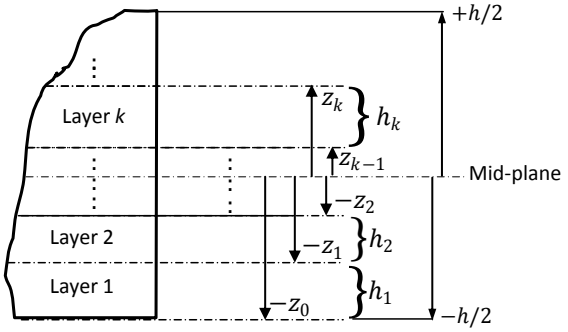

Figure 3: Sketch illustrating vertical geometry of a general laminate.
Figure 2.5 *Sketch illustrating vertical geometry of a general laminate*

Consequently, the bending-extension and bending stiffness coefficients can be determined as:

$$B_{ij} = \frac{1}{2}\sum_{k=1}^{L} \bar{Q}_{ijk}\, h_k \left(h_k + 2\sum_{i=1}^{k-1} h_i - h \right)$$
$$D_{ij} = \frac{1}{3}\sum_{k=1}^{L} \bar{Q}_{ijk} \left[h_k^3 + 3h_k \left(\sum_{i=1}^{k} h_i - h/2 \right) \sum_{i=1}^{k-1} h_i - h/2 \right) \tag{19}$$

The validity of equation (19) was confirmed by comparing with results obtained using equation (18) and Staab's expressions [18]. All three expressions produced exactly the same results for the Al/PVDF/PZT laminate used in the present impact analysis (see Table 1 for material properties).

3.2 Effective transverse properties of the trimorph plate

To calculate the constants of the contact model in Section 2.2, the Young's modulus, Poisson ratio and yield stress of the target in the transverse direction must be known. Since the trimorph plate is made up three different isotropic materials laminated together, effective properties are needed and cannot be obtained from available material properties data. An approximate analytical solution to the problem is the 'strength of materials' approach which has been applied in studying the low-velocity impact response of sandwich laminates [19] and functionally graded laminates [20], and verified experimentally for impact analysis [21]. The strength of materials approach is suitable for use under plane stress conditions, quasi-static loading and when the effect of the in-plane material properties of the target on the transverse deformation can be neglected [19]. These conditions apply to the impact of the trimorph plate; hence, strength of materials approach is considered to be appropriate for the present investigation. The effective transverse properties of the trimorph plate can be estimated as:

$$\begin{aligned} E_t &= h/(h_1/E_1 + h_2/E_2 + h_3/E_3) \\ v_t &= (v_1 h_1 + v_2 h_2 + v_3 h_3)/h \\ \rho_t &= (\rho_1 h_1 + \rho_2 h_2 + \rho_3 h_3)/h \\ S_y &= h/\left(h_1/S_{y1} + h_2/S_{y2} + h_3/S_{y3}\right) \end{aligned} \tag{20}$$

where $h = h_1 + h_2 + h_3$ is the total thickness of the plate; the subscript, t, represents the target which here is the plate; the subscripts 1, 2, and 3 represent the layers of the plate from bottom to top; h_k, E_k, v_k, ρ_k, and S_{yk} are the thickness, Young's modulus, Poisson's ratio, density and yield stress of the kth layer of the trimorph plate, respectively.

4 DISCUSSIONS OF RESULTS

4.1 Validation of modelling and solution approach

The impact model derived above have been solved by direct numerical integration using the NDSolve function in *Mathematica*™. To validate the modelling and solution approach used in the present analysis, a well-known impact problem first studied by Karas [22] is re-examined. This problem has been studied by many others including Goldsmith [2] and Abrate [1], and can be considered as a benchmark case. The impact event involves the elastic impact of a simply-supported square steel plate struck by a steel ball. The material and geometrical properties of the impact system are: properties of steel – ρ = 7806 [kg/m^3], E = 206.8 [GPa] and υ = 0.3 [-]; Plate dimensions = 0.2 × 0.2 × 0.008 [m^3]; Impactor diameter = 0.02 [m]; velocity = 1.0 [m/s]. The impactor mass was calculated to be 0.0327 [kg]. Since the impact is assumed to be elastic the Hertz contact model is used to estimate the impact force.

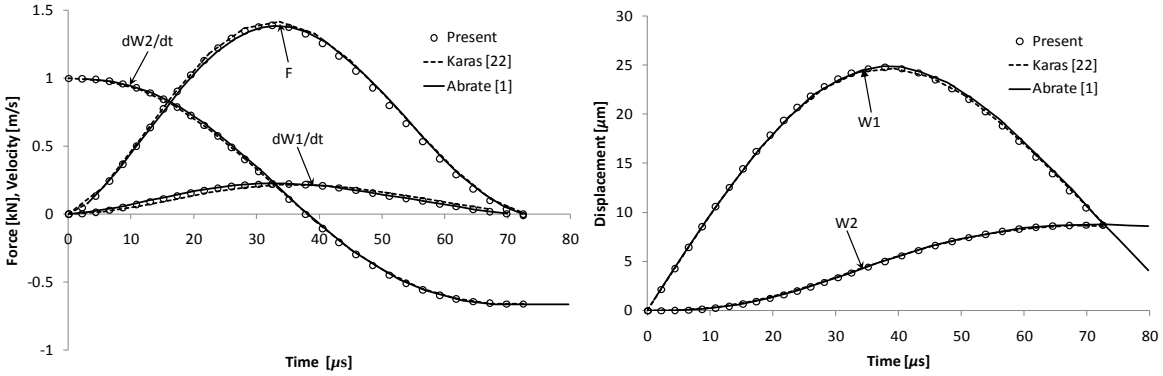

Figure 4: Impact response of a transversely flexible steel plate struck by a steel ball. F – force, dW1/dt – plate velocity, dW2/dt – impactor velocity, W1 – plate displacement, W2 – impactor displacement.

Karas [22] and Abrate [1] both used the complete modelling approach, but while the former solved the reduced models using small-increment integration scheme the latter employed the Newmark time integration scheme. The results obtained by Karas [22] and Abrate [1] and that of the present approach are compared in Figure 4, and all three methods are in good agreement. This shows that results obtained using the NDSolve function are reliable. Hence, the NDSolve function has been used to solve the elastoplastic impact models of the trimorph plate.

4.2 Elastoplastic impact analysis of Al/PVDF/PZT trimorph plate

A study of the elastoplastic impact response of a trimorph plate with layers arranged as Al/PVDF/PZT from top to bottom was carried out. The spherical surface of the impactor is in contact with the aluminium layer. The material and geometrical properties of the plate layers are shown in Table 1.

Material	ν [-]	E [GPa]	ρ [kg/m^3]	S_y [MPa]	h [mm]
Al	0.33	70	2700	320	3.0
PVDF	0.44	1.1	1770	50	1.0
PZT	0.3	64	7600	250	1.0

Table 1: Material and geometrical properties of the layers of the trimorph plate.

The other material and geometrical properties of the impact system are: $a = 100\ [mm]$; $b = 100\ [mm]$; $m_i = 1\ [kg]$; $V_0 = 0.30\ [m/s]$; $E_i = 210\ [MPa]$; $E_i = 7800\ [kg/m^3]$; $\nu_i = 0.30\ [-]$; $R_i = 10\ [mm]$. Impactor material: steel.

Effect of number of vibration modes used in the solution

The accuracy of the solution of the impact models depends on the number of vibration modes used in the solution. The impact force history was determined for different numbers of vibration modes as shown in Figure 5. The figure shows that nine vibration modes (i.e. $m = n = 5$) are sufficient to guarantee accurate results. Hence, the results presented and discussed in this section have been obtained using a nine mode approximation. In Figure 5, the blue lines represent the elastic loading response, the red lines represent the elastoplastic loading response, and the black lines represent the response when unloading from an elastoplastic loading stage. This colour definition has also been used in later figures.

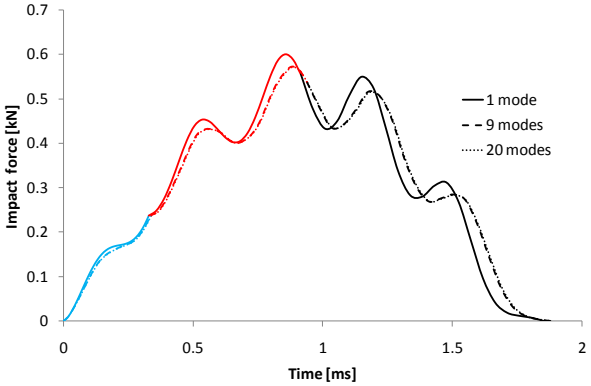

Figure 5: Effect of the number of vibration modes used in the solution of the impact model on the accuracy of the results obtained for the Al/PVDF/PZT plate.

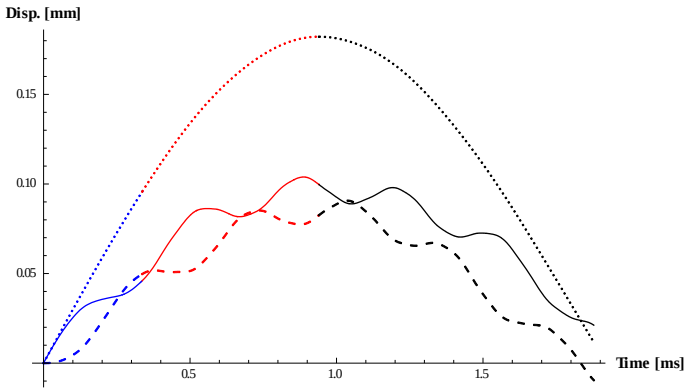

Figure 6: Displacement histories of Al/PVDF/PZT plate struck by steel impactor. Dotted line – impactor displacement, short-dash line – plate displacement, solid line – indentation.

Figure 6 shows the displacement histories during the elastoplastic impact response of the Al/PVDF/PZT plate. The displacement of the impactor is smooth whereas there are oscillations in the displacement of the plate giving rise to oscillations in the indentation. The response has a maximum indentation of 103.95 [μm], which occurs in the nonlinear elastoplastic loading stage, and a permanent indentation of 21.16 [μm]. The maximum contact force is 573.95 [N] and the impact duration is 1.88 [ms]. The loading ends when the velocity of the impactor is zero and this occurs when the time is 0.94 [ms] (see Figure 7). The results of the simulation shows that the point of maximum indentation (0.89 [ms], 103.95 [μm]) is

different from the end point of the impact loading (0.94 [ms], 99.7 [μm]), and this observation has also been reported previously by Abrate [1].

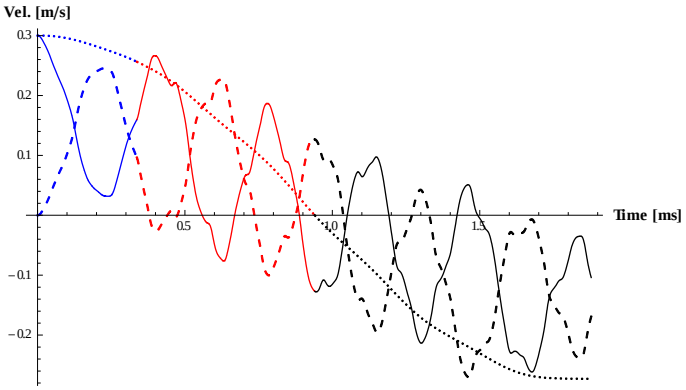

Figure 7: Velocity histories of Al/PVDF/PZT plate struck by steel impactor. Dotted line – impactor velocity, short-dash line – plate velocity, solid line – relative velocity.

Effect of contact model used to estimate the impact force

To investigate the effect of the contact model used to estimate the impact force on the response predicted, the results of three contact models (i.e. the present contact model, the contact model of Majeed et al [23] and the Hertz contact model) were compared. An initial impact velocity of 2.0 [m/s] was used in the simulations to ensure that the indentation response is well into the elastoplastic stage. The impact responses predicted by the three contact models are compared in Figure 8. The force histories predicted by all three contact models are in good agreement, demonstrating that the force history is not quite sensitive to the contact model used. However, the indentation history predicted by the Hertz contact model is different from that predicted by the elastoplastic contact models. The latter predict significant elastoplastic deformation with a permanent indentation at the end of the impact. The present contact model predicts a maximum indentation of 0.37 [mm] and a permanent indentation of 59.8 [μm], the contact model of Majeed et al [23] predicts 0.38 [mm] and 65.7 [μm] respectively, while the Hertz contact model predicts a maximum indentation of 0.34 [mm] and no permanent indentation. This shows that the contact model used for estimating the impact force of a large-mass impact can significantly affect the accuracy of the predictions and limit the information that can be obtained. This observation differs from the position taken by most investigators that the predicted response during large mass impact is insensitive to the contact model used to estimate the impact force [1]. Hence, the choice of contact model used to study large mass impact events is an important consideration.

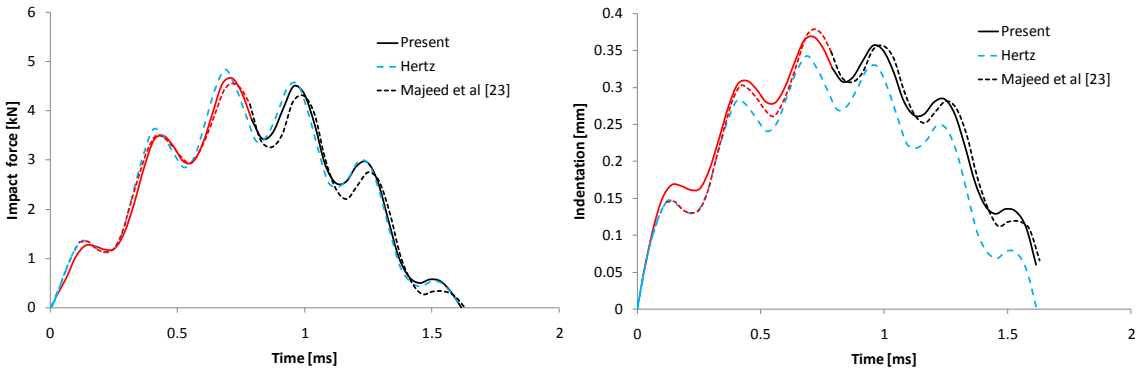

Figure 8: Impact response of Al/PVDF/PZT plate struck by steel impactor at an initial impact speed of 2.0 [m/s].

5 ACTIVE IMPACT DAMAGE MITIGATION

Piezoelectric actuation can be used to alter the effective transverse stiffness (flexibility) of a structure by creating a pre-stress to make it apparently stiffer or more compliant [24]. The effective transverse stiffness of a plate with piezoelectric layer actuation is the sum of the mechanical bending stiffness and the induced piezoelectric stiffness. The latter may be positive or negative, depending on whether the induced in-plane piezoelectric stress is tensile or compressive. Studies [6] on the effect of flexibility on the impact response of a plate showed that the impact response of the plate is significantly influenced by altering its flexibility. This means that a plate with piezo-actuator layers can be used to influence its impact response to a rigid blunt projectile by actively inducing a state of pre-stress in the plate. This idea can be exploited to actively mitigate blunt object impact damage.

A few studies have attempted to investigate the application of piezo-actuation during impact [7, 8], but these studies applied active bending and damping induced by piezo-actuation to investigate the control of low-velocity impact response. In this section, a parametric study is carried out to demonstrate that the flexibility of a trimorph plate, which can be altered using active pre-stressing induced by piezo-actuation, could be exploited to mitigate impact damage effects. To achieve this, a parameter, α, used to alter the effective transverse stiffness of the trimorph plate without changing the dimensions or material properties of the plate (as would be expected during active pre-stressing induced by piezo-actuation) is introduced into the transverse vibration model as shown in equation (21). The parameter, α, represents the percentage change in the effective transverse stiffness of the plate. When $\alpha < 0$, the plate is apparently less flexible and when $\alpha > 0$, the plate is apparently more flexible. The normal case is represented by $\alpha = 0$ when the effective transverse stiffness is determined by the mechanical bending stiffness only.

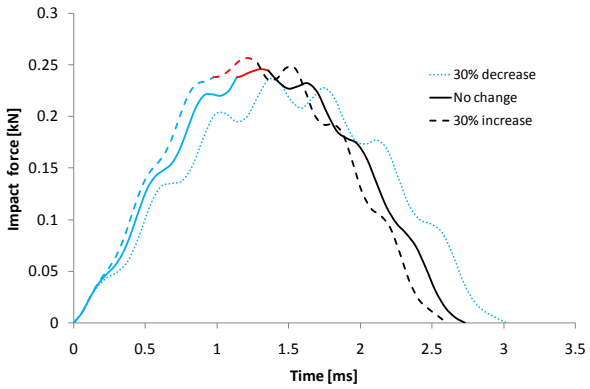

Figure 9: Influence of transverse flexibility on the elastoplastic impact response of Al/PVDF/PZT plate.

$$\ddot{W}_{mn}\} + K(1-\alpha)\{W_{mn}\} = F(t)\{\gamma_{mn} \tag{21}$$

Figure 9 shows the effect of α on the impact response of the Al/PVDF/PZT plate. In this figure, the mass of the impactor is 2.0 [kg] and the impact velocity is 0.10 [m/s]. Three cases are considered i.e. $\alpha = 0$, $\alpha = -0.3$, and $\alpha = 0.3$. The reference point is taken when the effective stiffness is equal to the mechanical stiffness, i.e. $\alpha = 0$. For $\alpha = 0$, the maximum impact force is 246.15 [N], the impact duration is 2.73 [ms] and the permanent indentation is 3.36 [μm]. When $\alpha = -0.3$, the effective stiffness is 30% higher than normal ($\alpha = 0$) and the impact response, which is more localised, is characterised by a higher maximum impact force (263.45 [N]), shorter impact duration (2.60 [ms]) and larger permanent indentation (5.10 [μm]). For $\alpha = 0.3$, the effective stiffness is 30% lower than normal and the response has become purely elastic with no permanent indentation. The maximum impact force is about

4.0% lower than for $\alpha = 0$ and the impact duration is longer (3.02 [ms]). The implication is that an impact, which should ordinarily result in a permanent indentation, can be converted to one with no permanent indentation. This result is significant because it demonstrates that alteration of the effective stiffness of the plate could be exploited to either reduce or completely eliminate elastoplastic impact effects.

6 CONCLUSIONS

The elastoplastic impact response of a transversely flexible trimorph plate struck by a spherical impactor has been investigated analytically. The investigations reveal that the contact model used to predict the impact force of a large mass impact event can significantly affect the resulting predictions, and also limit detailed description of the impact response. Also, investigations on the effect of transverse flexibility on the impact response of the trimorph plate showed that elastoplastic impact effects could be reduced significantly or eliminated by altering the effective transverse stiffness of the plate; an observation that could be exploited for active impact control to mitigate impact damage.

ACKNOWLEGDEMENT

The first author is grateful to the Commonwealth Scholarship Commission (CSC), UK for funding his PhD research (CSC Award Ref: NGCA-2011-60), of which this work is a part.

REFERENCES

[1] S. Abrate, *Impact on composite structures*. Cambridge University Press, 1998.

[2] W. Goldsmith, *Impact: The theory and physical behaviour of colliding solids*. Dover Publications, 2001.

[3] S. Abrate, Modeling of impacts on composite structures. *Computers and Structures*, **51**, 129 – 138, 2001.

[4] C. Zener, The intrinsic inelasticity of large plates. *Physical Review*, **59**, 669 – 673, 1941.

[5] A.P. Christoforou, S.R. Swanson, Analysis of impact response in composite plates. International Journal of Solids and Structures, **27 (2)**, 161 – 170, 1991.

[6] A.P. Christoforou, A.S. Yigit, Effect of flexibility on low velocity impact response. *Journal of Sound and Vibration*, **217 (3)**, 563 – 578, 1998.

[7] A.S. Yigit, A.P. Christoforou, Control of low-velocity impact response on composite plates. *Journal of Vibration and Control*, **6**, 429 – 447, 2000.

[8] D.A. Saravanos, A.P. Christoforou, Impact response of adaptive piezoelectric laminated plates. *AIAA Journal*, **40(10)**, 2087 – 2095, 2002.

[9] D. Zheng, W.K. Binienda, Effect of permanent indentation on the delamination threshold for small mass impact on plates. *International Journal of Solids and Structures*, **44**, 8143 – 8158, 2007.

[10] A. Big-Alabo, M.P. Cartmell, Vibration analysis of a trimorph plate for optimised damage mitigation. *Journal of Theoretical and Applied Mechanics*, **49 (3)**, 641 – 664, 2011.

[11] R. Szilard, *Theory and Applications of Plate Analysis: Classical, Numerical and Engineering Methods*. John Wiley & Sons Inc., 2004.

[12] A. Big-Alabo, P. Harrison, M.P. Cartmell, Elastoplastic half-space impact analysis using a novel contact model that accounts for post-yield effects. A. Cunha, E. Caetano, P. Ribeiro, G. Müller (eds.). *9th International Conference on Structural Dynamics (EURODYN 2014)*, Porto, Portugal, 30 June - 2 July, 2014.

[13] A. Big-Alabo, P. Harrison, M.P. Cartmell, Contact model for elastoplastic analysis of half-space indentation by a spherical impactor. *Computers and Structures*, **151**, 20 – 29, 2015.

[14] K.L. Johnson, *Contact mechanics*. Cambridge University Press, 1995.

[15] L.Y. Li, C.Y. Wu, C. Thornton, A theoretical model for the contact of elastoplastic bodies. *Proc. IMechE, Part C: Journal of Mechanical Engineering Science*, **216**, 421 – 431, 2002.

[16] R. Hill, B. Storakers, A.B. Zdunek, A theoretical study of Brinell hardness test. *Proceedings of Royal Society London A*, **423**, 301 – 330, 1989.

[17] O. Bartier, X. Hernot, G. Mauvoisin, Theoretical and experimental analysis of contact radius for spherical indentation. *Mechanics of Materials*, **42**, 640–656, 2010.

[18] G.H. Staab, *Laminar composites*. Butterworth Heinemann, 1999.

[19] M.R. Khalili, K. Malekzadeh, R.K. Mittal, Effect of physical and geometrical parameters on the transverse low-velocity impact response of sandwich panels with a transversely flexible core. *Composite Structures*, **77**, 430 – 443, 2007.

[20] M. Shariyat, F. Farzan, Nonlinear eccentric low-velocity impact analysis of highly prestressed FGM rectangular plate, using a refined contact law. *Archive of Applied Mechanics*, **83**, pp 623–64, 2013.

[21] R.A. Larson, A.N. Palazotto, Property estimation in FGM plates subject to low-velocity impact loading. *Journal of Mechanics of Materials and Structures*, **4 (7-8)**, 1429 – 1451, 2009.

[22] K. Karas,: Platten unter seitchem stoss. *Ingenieur Archiv*, **10**, 237-250, 1939.

[23] M.A. Majeed, A.S. Yigit, A.P. Christoforou, Elastoplastic contact/impact of rigidly supported composites. *Composites: Part B*, **43**, 1244 – 1251, 2012.

[24] H. Waisman, H. Abramovich, Active stiffening of laminated composite beams using piezoelectric actuators. *Composites Structures*, **58**, 109 – 120, 2002.